Quantitative Structure−Activity Relations for γδ T Cell Activation by Phosphoantigens

William Gossman and Eric Oldfield*

*Department of Chemistry, University of Illinois at Urbana-Champaign, 600 South Mathews Avenue, Urbana, Illinois 61801*

γδ T cells help contribute to innate immunity and are activated by the natural phosphoantigens produced by the organisms responsible for causing, for example, tuberculosis, malaria, tularemia, and plague. They are also activated by synthetic phosphoantigens and are cytotoxic to tumor cells. Here, we show that it is now possible to accurately predict γδ T cell activation by both natural and synthetic phosphoantigens by using the quantitative structure−activity relationship (QSAR) techniques commonly used in drug design. This approach should be of use in developing novel immunotherapeutic agents as well as contributing to a better understanding of the immune system's response to infectious agents.

Introduction

There is currently intense interest in investigating the activation of γδ T cells by small molecules for potential use in the pharmacologist's armamentarium,[1,2] since these T cells are thought to contribute to innate immunity in humans and other primates.[3] They comprise 5% of the normal T cell population, but this can increase to up to ~80% on infection with a broad range of pathogens, such as those responsible for tuberculosis,[4−7] malaria,[8] and tularemia.[9] These immediately reactive human γδ T cells express Vγ2Vδ2 (also known as Vγ9Vδ2) T cell antigen receptors (TCRs), which are involved with the recognition of a broad variety of small molecule "phosphoantigens" produced by many bacteria and protozoa. These potently expand γδ T cell populations, leading to rapid production of IFN-γ and TNF-α. Another class of phosphoantigens, bisphosphonates, is also known to expand γδ T cell populations[10] and has been shown to have potent antitumor activity,[11−13] as do other synthetic phosphoantigens.[14] The structural basis for this innate cellular immunity involves the γδ T cell receptor,[15] and over 70 compounds have now been shown to expand γδ T cell populations.[1,13,14,16−19] However, there have been no reports of quantitative structure−activity relationships (QSARs) for this immune response. Here, we show that the three-dimensional (3D) QSAR techniques routinely used in drug design can also be used to predict the activities of a broad range of antigens within a factor of ~4 over a range in activity of ~3 × 10^6, opening the way to the rational design of novel immunotherapeutic agents.

γδ T cells expressing Vγ2Vδ2 TCRs respond to many infectious agents, including *Mycobacterium* spp., *Pseudomonas aeruginosa*, *Salmonella* spp., *Escherichia coli*, *Plasmodium falciparum*, *Francisella tularensis*, *Yersinia* spp., etc., and these responses have been associated with the production of a series of so-called phosphoantigens by these organisms.[9,20−24] These compounds are all thought to be small molecule pyrophosphate

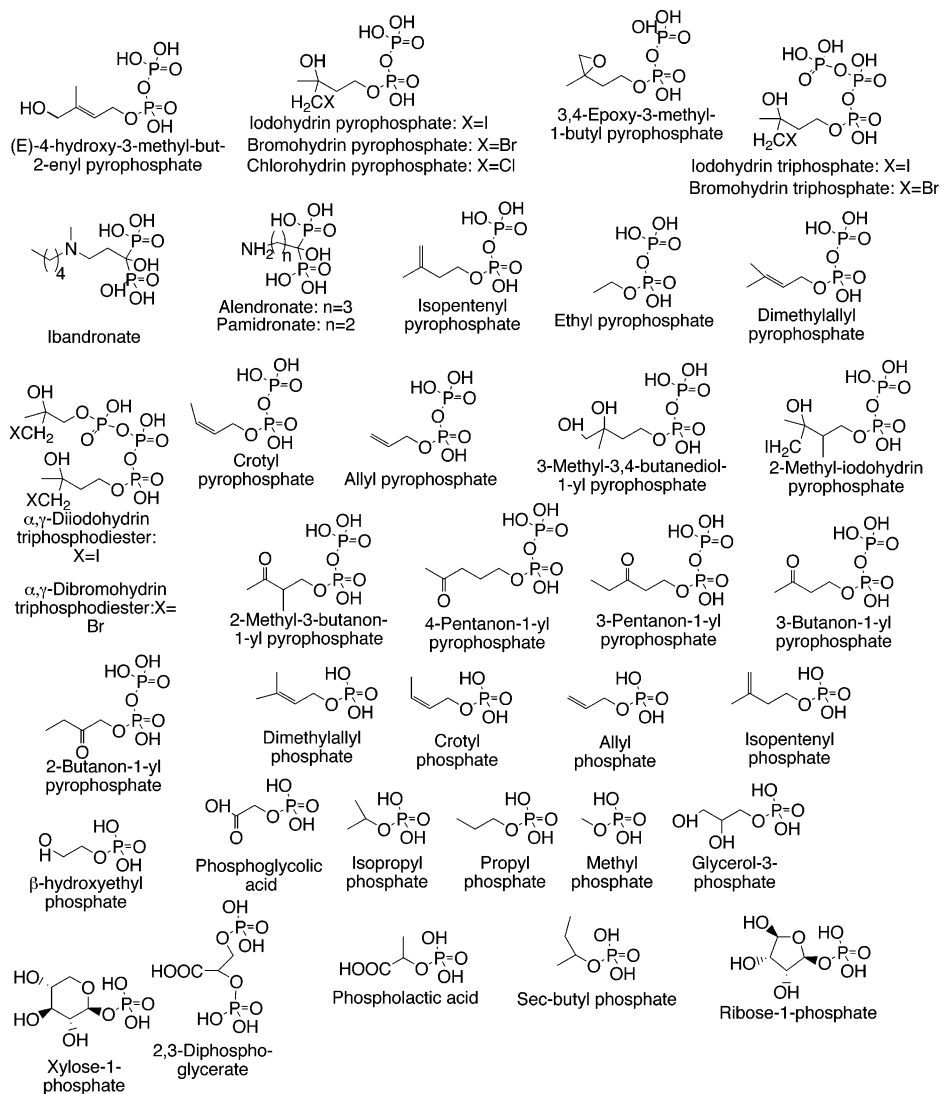derivatives, shown generically below in **1** where Y, X, P, and N are variables.
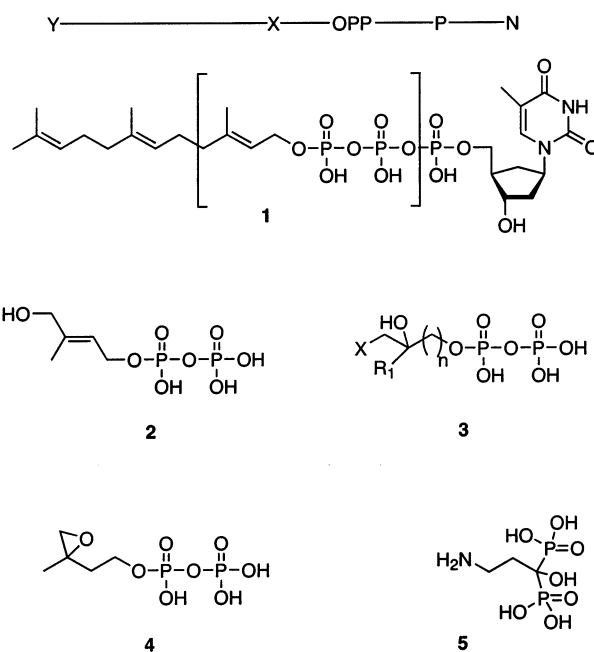
Phosphoantigens were first detected in *Mycobacterium tuberculosis* extracts, and to date, the most active species found is **2** ((*E*)-4-hydroxy-3-methyl-but-2-enyl pyrophosphate), having a 4 × 10^−10 M EC$_{50}$ [25] and identified as a product of the alternative mevalonate pathway in *E. coli*.[24] A variety of synthetic analogues of **2**, such as **3** and **4**, have been described in the literature and also have very low EC$_{50}$ values (~0.5−100 nM for **3** and **4**) and are of interest in the context of the treatment of non-Hodgkin's B lymphoma, multiple myeloma, and autologous cell therapy of renal carcinoma. A third class of synthetic phosphoantigens, the bisphosphonates, currently used in bone resorption therapy, have also been shown to expand γδ T cell populations[13] and to have anticancer as well as antibacterial activity.[3,10] For example, the 1,1-bisphosphonate pamidronate (**5**) can activate Vγ2Vδ2 T cells

---

* To whom correspondence should be addressed. Tel: 217-333-3374. Fax: 217-244-0997. E-mail eo@chad.scs.uiuc.edu.
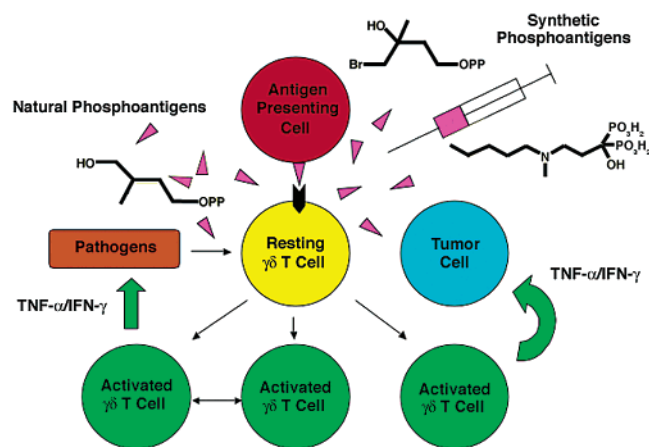
Figure 1. Schematic illustration of some of the interactions between γδ T cells and pathogens mediated by natural phosphoantigens and between γδ T cells and tumor cells mediated by synthetic phosphoantigens. The full molecular details of phosphoantigen presentation are not known. In tuberculosis, there appears to be bacterial killing mediated by TNF-α/IFN-γ. In tularemia, antigen production appears to result in γδ T cell self-cytotoxicity. Some synthetic antigens have been shown to have both antibacterial and antitumor activity.

leading to control of both *E. coli* and *Proteus morganii* infections in vivo.[3] A schematic illustration of some of the interactions between infectious agents and γδ T cells mediated by natural phosphoantigens and TNF-α/IFN-γ, together with the corresponding synthetic phosphoantigen/γδ T cell/tumor cell interaction, is outlined in Figure 1.

Materials and Methods

To begin to relate the γδ T cell stimulation activity of both natural and synthetic phosphoantigens to their 3D chemical structures, we have used two computational chemistry methods commonly used in drug design: comparative molecular field analysis (CoMFA)[26] and pharmacophore modeling.[27] The CoMFA method calculates interaction energies between a molecule and a series of probes (electrostatic, hydrogen bonding, and hydrophobic) and correlates variances in the interaction energies with activity, while pharmacophore modeling (using the Catalyst program) correlates activity with the presence of particular spatial distributions of chemical features (such as hydrogen bond donors, negative ionizable groups, etc). Both approaches permit predictions of drug activity and have recently been successfully applied to bisphosphonates.[28,29]

Results and Discussion

We show in Figure 2 the structures of the phosphoantigens investigated. The compound names (the trivial

Figure 2. Structures and names of compounds investigated.

Table 1. Experimental EC_{50} and pEC_{50} and Predicted pEC_{50} Values for $\gamma\delta$ T Cell Activation

compd[a]	experimental activity[b]		CoMFA predicted pEC_{50}[c]					Catalyst predicted pEC_{50}[c]				
	EC_{50} (μM)	pEC_{50}	training set	four compd test set				training set	four compd test set			
(E)-4-hydroxy-3-but-enyl PP	0.0004	9.30	9.17	9.21	9.16	9.16	9.13	7.60	7.54	7.49	7.54	7.51
iodohydrin PP	0.0012	8.91	7.54	7.63	7.51	7.48	**7.28**	7.29	7.60	7.39	7.46	**7.46**
bromohydrin PP	0.0100	8.00	7.54	7.64	7.52	**7.49**	7.29	7.26	7.47	7.59	**7.38**	7.51
chlorohydrin PP	0.0707	7.15	7.54	7.64	7.51	7.48	7.28	6.82	7.07	7.21	7.15	7.29
iodohydrin PPP	0.224	6.65	7.24	**7.34**	7.21	7.18	6.99	6.74	**7.00**	7.04	6.80	6.85
bromohydrin PPP	0.346	6.46	7.25	7.35	7.22	7.19	7.00	6.41	6.49	6.43	6.14	6.37
3,4-epoxy-3-methyl-1-butyl PP	0.400	6.40	6.12	6.16	**6.05**	6.08	6.12	5.66	5.64	**5.51**	5.55	5.62
alendronate	0.900	6.05	5.11	5.14	5.09	5.08	5.12	5.55	5.47	5.21	5.48	5.34
ibandronate	1.00	6.00	5.44	5.48	5.35	5.40	5.48	6.59	6.30	6.14	6.29	6.00
isopentenyl PP	3.16	5.50	5.25	5.27	5.23	5.22	**5.26**	5.59	5.60	5.51	5.52	**5.60**
ethyl PP	3.16	5.50	5.17	5.19	5.16	5.14	5.19	5.57	5.62	5.52	5.59	5.59
dimethylallyl PP	3.16	5.50	5.68	**5.72**	5.60	5.64	5.72	5.49	**5.64**	5.44	5.54	5.60
crotyl PP	3.16	5.50	5.27	5.29	5.26	5.24	5.28	5.68	5.70	5.55	5.62	5.66
allyl PP	3.16	5.50	5.25	5.27	**5.23**	5.22	5.26	5.68	5.62	**5.54**	5.59	5.62
3-methyl-3,4-butanediol-1-yl PP	3.16	5.50	5.59	5.63	5.51	5.55	5.64	5.60	5.54	5.46	5.49	5.55
pamidronate	5.66	5.25	4.99	5.01	4.97	**4.96**	5.01	5.55	5.43	5.19	**5.48**	5.36
2-methyl-iodohydrin PP	7.07	5.15	4.85	4.89	4.85	4.85	**4.65**	5.70	5.85	6.30	5.70	**6.74**
α,γ-diiodohydrin PPPDE	8.66	5.06	5.30	5.33	5.30	5.30	5.09	5.66	5.68	5.64	5.59	5.72
α,γ-dibromohydrin PPPDE	14.1	4.85	5.33	5.36	5.33	5.33	5.12	6.11	5.62	5.54	5.62	5.62
2-methyl-3-butanon-1-yl PP	31.6	4.50	4.43	**4.45**	4.48	4.43	4.20	4.74	**4.80**	4.57	4.66	4.77
4-pentanon-1-yl PP	31.6	4.50	5.17	5.18	5.15	5.14	5.19	3.37	3.27	3.22	3.07	3.36
3-pentanon-1-yl PP	31.6	4.50	5.24	5.26	5.22	**5.21**	5.26	5.62	5.66	5.54	**5.59**	5.62
3-butanon-1-yl PP	40.0	4.40	5.24	5.26	5.22	5.21	5.26	3.37	3.27	3.22	3.07	3.36
2-butanon-1-yl PP	44.7	4.35	5.12	5.14	5.11	5.09	**5.15**	5.72	5.66	5.49	5.52	**5.64**
dimethylallyl P	158	3.80	3.51	3.47	3.46	3.54	3.60	3.62	3.77	3.92	3.85	3.85
crotyl P	158	3.80	3.51	3.47	**3.46**	3.54	3.59	3.49	3.74	**3.89**	3.85	3.82
allyl P	158	3.80	3.08	3.03	3.11	3.13	3.14	3.37	3.57	3.70	3.66	3.60
isopentenyl P	158	3.80	3.51	**3.48**	3.47	3.55	3.60	3.37	**3.44**	3.60	3.55	3.49
β-hydroxylethyl P	224	3.65	3.02	2.97	3.03	3.06	3.10	3.36	3.27	3.43	3.30	3.35
phosphoglycolic acid	707	3.15	3.11	3.05	3.13	**3.15**	3.17	3.37	3.27	3.22	**3.07**	3.36
isopropyl P	707	3.15	3.10	3.05	3.12	3.14	3.16	3.36	3.33	3.43	3.40	3.40
propyl P	707	3.15	3.09	3.04	**3.11**	3.13	3.15	3.37	3.43	**3.55**	3.49	3.55
methyl P	707	3.15	3.04	2.98	3.06	3.08	3.10	1.37	1.33	1.59	1.31	1.54
glycerol-3-P	1580	2.80	3.55	3.52	3.51	3.59	**3.64**	3.36	3.68	3.70	3.74	**3.85**
xylose-1-P	1580	2.80	3.40	3.35	3.36	3.44	3.52	3.36	3.59	3.77	3.54	3.55
2,3-diphosphoglycerate	1580	2.80	2.60	**2.55**	2.60	2.63	2.67	3.37	**3.26**	3.22	3.07	3.36
phospholactic acid	1580	2.80	3.03	2.98	3.05	3.07	3.09	3.37	3.27	3.22	3.07	3.36
sec-butyl P	2240	2.65	3.03	2.98	3.04	**3.07**	3.09	3.37	3.48	3.60	**3.55**	3.59
ribose-1-P	3160	2.50	2.88	2.82	**2.89**	2.92	2.98	3.64	3.41	**3.84**	3.54	3.55
R^2[d]			0.91	0.91	0.90	0.90	0.93	0.80	0.80	0.80	0.80	0.82
F_{test}[e]			84.8	70.4	66.5	63.2	93.9					
R^2_{cv}[f]			0.87	0.86	0.85	0.84	0.86					
R^2_{bs}[g]			0.91	0.91	0.90	0.90	0.93					
n[h]			5	5	5	5	5	4	4	4	4	4
N[i]			39	34	34	34	34	39	34	34	34	34

[a] Notations: PP = pyrophosphate; PPP = triphosphate; PPPDE = triphosphodiester; P = phosphate. [b] From ref 17, geometric mean values shown when a range given. The data for **2** are from ref 25. [c] Bold values represent predicted activities of compounds that were not included in the training set. [d] Correlation coefficient. [e] Ratio of R^2 explained to unexplained = $R^2/(1 - R^2)$. [f] Cross-validated correlation coefficient after leave-one-out procedure. [g] Average squared correlation coefficient calculated during the validation procedure. [h] Optimal number of principal components (CoMFA) or number of components in Catalyst pharmacophore hypothesis. [i] Number of observations.

names used in ref 17) are also shown. The compounds are ordered in terms of increasing EC_{50}, left to right and top to bottom. The corresponding EC_{50} values for T cell activation (in micromolar) for these compounds are given in Table 1, where average EC_{50} (or $pEC_{50} = -\log EC_{50}$ (M)) values are used when a range is given in the original compilation of Espinosa et al.[17] While there are expected to be small differences in the ED_{50} values determined by different groups when using different techniques (cell proliferation, IFN-γ or TNF-α production) as well as the use of different clones, we have found that where data have been reported from more than one group, there is good agreement. For example, we find EC_{50} values of 3, 3, 3, and 10 μM for stimulation by isopentenylpyrophosphate (refs 30–32 and 16, respectively). Likewise, for pamidronate, Das et al.[10] found EC_{50} values in the $\sim$1–10 μM range (using IL-2, IFN-

γ, and %CD3 expansion assays) in good accord with the 4 μM EC_{50} value found by Kunzmann et al.[13]

Structures were generated for CoMFA investigation by using steepest descents followed by conjugate gradient, and then Newton–Raphson algorithms for geometry optimization, with no constraints on the internal geometry of the molecules.[26] Each molecule was aligned to one of the most active molecules studied, iodohydrin pyrophosphate, acting as a template by performing an rms fitting of the pharmacophoric atoms of each conformer to those of the template using a shape reference alignment function. The alignments of each structure, obtained through pairwise superpositioning using the maximum common subgroup method, placed all 39 structures in the same reference frame as the shape reference compound. The enantiomers chosen were those that best fit the overall alignment. The aligned
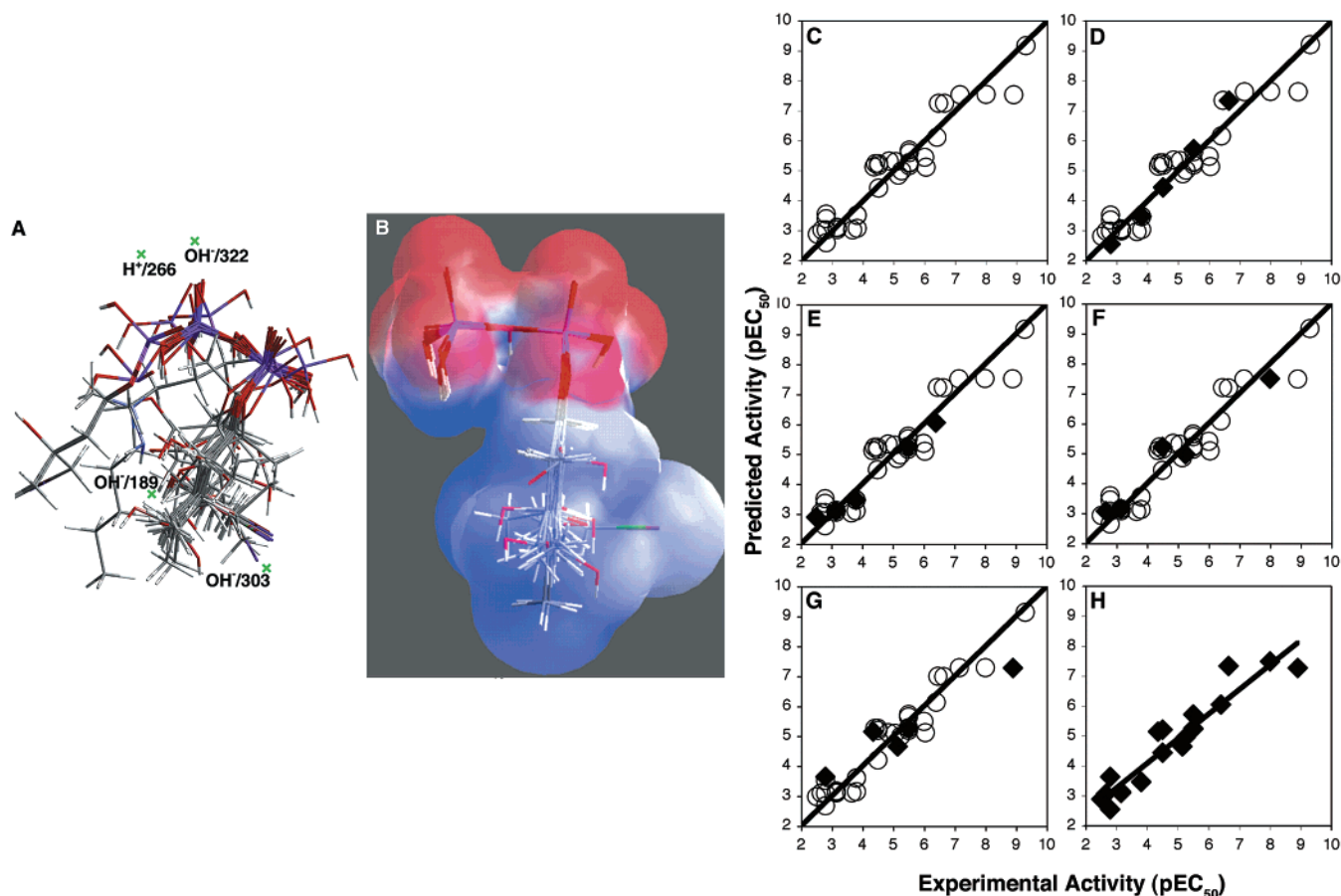
Figure 3. CoMFA results for $\gamma\delta$ T cell activation. (A) Alignment of all 39 compounds investigated. The descriptors are indicated ($N = 39$ compound training set). (B) Pseudoreceptor surface enclosing 21 mono- and pyrophosphates. (C)−(H), graphs of CoMFA-derived QSAR predictions for $\gamma\delta$ T cell activation vs experimental activity. (C) A 39 compound training set. (D−G) As in panel C but 34 compound training set (○) and 5 compound test set (◆) predictions. The numerical and statistical results are given in Table 1. The lines represents the ideal slopes of 1. (H) Composite 20 compound test set, for which the R^2 was 0.90 and the rms error in pEC_{50} was 0.57 (about a factor of four error in prediction over the 3×10^6 range in activity). Most of the experimental data is reported with a $10\times$ range for the EC_{50} and contributes to the error.

set of structures is shown in Figure 3A. We then used CoMFA techniques to analyze the inhibition data shown in Table 1. We first performed a regression analysis of the inhibition results by using a genetic function approximation (GFA) algorithm[33] to obtain the following QSAR equation:

$$pEC_{50} = 3.31 + 0.01 \times \text{“}OH^-/189\text{”} +$$
$$0.06 \times \text{“}OH^-/303\text{”} + 0.11 \times \text{“}OH^-/322\text{”} +$$
$$0.07 \times \text{“}H^+/266\text{”} \quad (1)$$

where the descriptors, OH^-, define the corresponding probe interaction energies between a hydrogen bond donor/acceptor and the molecule of interest at the specified grid points. The descriptor, H^+, is the interaction energy between a proton (H^+) and the molecule and gives the electrostatic potential energy of interaction. Charges were calculated by using the Gasteiger method.[34] The locations of the descriptors in eq 1 are also shown in Figure 3A. The optimal number of components in the final GFA model was determined by cross-validated R^2 [35] and standard error prediction values, as obtained from the leave-one-out cross-validation technique. The GFA analysis gave a correlation coefficient of 0.91 with a cross-validated R^2_{cv} of 0.87 and an optimal number of components of five (one fixed term plus four variables).

To obtain statistical confidence limits, the noncross-validated analysis was repeated with 10 bootstrap groups, which yielded an R^2_{bs} of 0.91.[35] Cross-validation provides information concerning the predictive ability of the QSAR data set by minimizing the occurrence of chance correlations in the QSAR model, and the boot-strapped R^2_{bs} value of 0.91 indicates a high degree of confidence in the analysis. Experimental and predicted pEC_{50} values with this training set and the associated statistical results are shown in Table 1 and graphically in Figure 3C.

These results are of interest since they indicate that it should be possible to predict EC_{50} values for $\gamma\delta$ T cell activation in a straightforward manner from 3D chemical structures. The experimental range of activity (EC_{50}) varies from ~400 pM for **2** to ~3 mM for ribose-1-phosphate, as shown in Table 1. So, to test the predictive ability of the CoMFA approach, we next carried out four sets of test calculations in which we deleted at random five (test set) points from the initial training set. The QSAR equations were then recomputed, and the results obtained were used to calculate the pEC_{50} values for the five compounds in each of the four test set calculations. The four sets of predicted pEC_{50} values are shown in bold in Table 1, as are the R^2, R^2_{cv}, R^2_{bs}, and F-test statistical results for each QSAR equation. The new
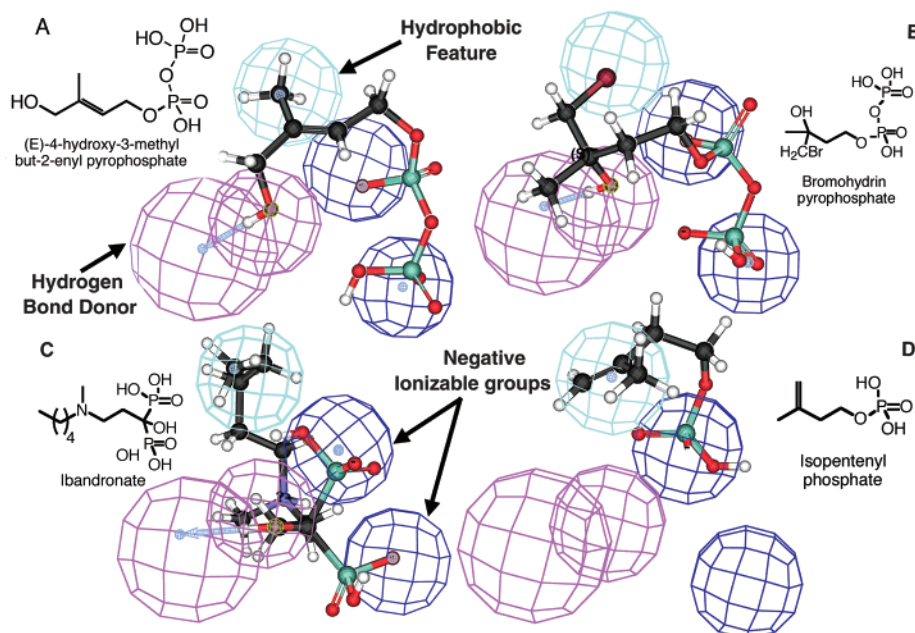
Figure 4. Catalyst pharmacophore hypothesis superimposed on four molecules having different activities. The features in each case are dark blue sphere, negative ionizable group; purple sphere, hydrogen bond donor; cyan sphere, hydrophobic feature. The molecules are (A) (*E*)-4-hydroxy-3-methyl-but-2-enyl pyrophosphate, (B) bromohydrin pyrophosphate, (C) ibandronate, and (D) isopentenyl phosphate.

QSAR/CoMFA equations were all virtually identical to the original model derived from the 39 compound training set. There is in general excellent agreement between the pEC_{50} predictions for the test set compounds (Table 1, ◆ in Figure 3D–G) and the experimentally observed values, with an rms error of 0.57 and an R^2 value of 0.90 for the 20 predicted compound pEC_{50} values (Figure 3H). These results show that it is now possible to predict pEC_{50} values for $\gamma\delta$ T cell activation within about a factor of four (rms error on $pEC_{50} = 0.57$) covering an experimental range in activity of $\sim 3 \times 10^6$. On the basis of the QSAR/CoMFA equations, it is also apparent that the interaction resulting in $\gamma\delta$ T cell activation is primarily polar in nature. The computed pseudoreceptor surface is shown in Figure 3B (together with 21 pyrophosphate and monophosphate molecules) and can be readily docked into the putative phosphoantigen binding site of the TCR,[36] as noted previously for the docking of **2**.[24]

While all of these R^2 and *F*-test values are very good, we felt it would nevertheless be desirable to validate these results by using a second, independent QSAR method, covering a large range of conformational space. We therefore used the Catalyst approach[27] in which up to 256 conformations of each molecule can be investigated, to develop a series of pharmacophore hypotheses. The five top-scoring hypotheses were very similar, and one such hypothesis is illustrated in Figure 4A–D. There are four components: two negative ionizable groups (e.g., two pyrophosphate phosphates or two phosphonates), a H-bond donor (e.g., the OH group in **2** or **3**), and a hydrophobic feature (e.g., a methyl group in **2** or the bromine atom in **3**). The presence of all four Catalyst features in the appropriate relative geometry results in very low EC_{50} values: less features correlate with less antigenic activity. For example, the most potent natural phosphoantigen **2** contains two negative ionizable groups (in the pyrophosphate moiety) as does

the drug phosphostim (**3**, X = Br), together with a hydrogen bond donor (the OH group) and a hydrophobic feature (the methyl group). In the synthetic phosphoantigen **3**, an OH group is again present, together with another hydrophobic feature, a bromine atom, as can be seen in Figure 4A,B. The $\gamma\delta$ T cell stimulatory activity of the bisphosphonate drug, ibandronate (bondronate) correlates with the presence once again of all four features, but here, the two phosphates are replaced by phosphonate groups (Figure 4C). Compounds with less features have less activity; for example, the weak activity of isopentenyl phosphate (observed $pIC_{50} = 3.80$, computed $pIC_{50} = 3.44$) correlates with the presence of only two pharmacophore features, a hydrophobic feature and a negative ionizable group (Figure 4D). Using this Catalyst hypothesis, we obtained the training set results shown in Table 1 ($R^2 = 0.80$). We then reinvestigated the training/test set prediction approach outlined above for the CoMFA method, and the training/test set results for four N = 34 (training)/N = 5 (test set) results are again shown in Table 1 and graphically in Figure 5. The overall (N = 20, Figure 5G) rms error for the predicted pEC_{50} values was 0.82 (corresponding to a factor of ~ 7 error in EC_{50} prediction). This result is slightly worse than that obtained by using the CoMFA approach but is still very good given that the overall range in activity investigated is $\sim 3 \times 10^6$ and most experimental EC_{50} values cover a $10\times$ range.

The ability to predict $\gamma\delta$ T cell activation from molecular structure within, on average, about a factor of four over a $>10^6$ range by using the CoMFA approach should facilitate the design or discovery of additional molecules of this type and represents the first application of 3D QSAR techniques to unraveling some of the details of the structural basis of innate immunity. This can be expected to be of interest in investigating a broad range of infectious diseases where $\gamma\delta$ T cell responses are involved, such as malaria, tuberculosis, tularemia,
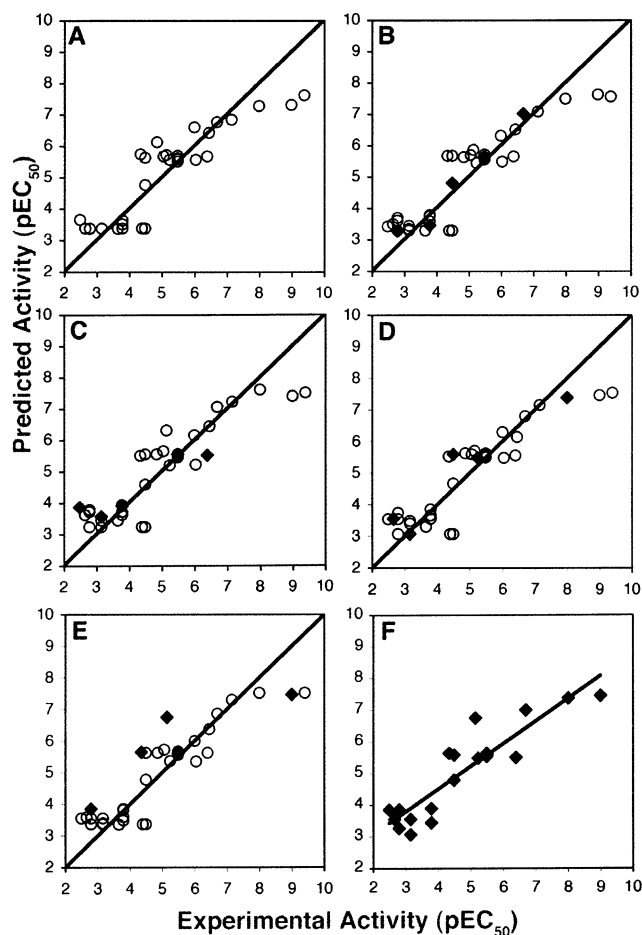
Figure 5. Graphs of Catalyst pharmacophore predictions of $\gamma\delta$ T cell activation vs experimental activity. (A) A 39 compound training set. (B−E) As in panel A but 34 compound training set (○) and 5 compound test set (◆) predictions. The numerical and statistical results are given in Table 1. The lines represent the ideal slopes of 1. (F) Composite 20 compound test set, for which the R^2 was 0.82 and the rms error in pEC_{50} was 0.82 (about a factor of seven error in prediction over the 3×10^6 range in activity).

and plague. In addition, the stimulation of $\gamma\delta$ T cells by synthetic phosphoantigens also offers considerable potential for cancer and human immunodeficiency virus immunotherapy[37] and potentially for vaccine development.[38] The QSARs we have described above can therefore be expected to be of widespread utility in developing new immunotherapeutic agents in much the same way that QSAR techniques are used to guide the development of other drugs.

Note Added after ASAP Posting. This manuscript was released ASAP on 9/19/2002 with an error in the Introduction. The correct version was posted on 9/27/2002.

References

(1) Hayday, A. C. $\gamma\delta$ Cells: A Right Time and a Right Place for a Conserved Third Way of Protection. *Annu. Rev. Immunol.* **2000**, *18*, 975−1026.

(2) Bendelac, A.; Bonneville, M. Autoreactivity by Design: Innate B and T Lymphocytes. *Nat. Rev. Immunol.* **2001**, *1*, 177−185.

(3) Wang, L.; Kamath, A.; Das, H.; Li, L.; Bukowski, J. F. Antibacterial Effect of Human Vγ2Vδ2 T Cells in vivo. *J. Clin. Invest.* **2001**, *108*, 1349−1357.

(4) Constant, P.; Poquet, Y.; Peyrat, M.-A.; Davodeau, F.; Bonneville, M.; et al. The Antituberculous *Mycobacterium bovis* BCG Vaccine Is an Attenuated Mycobacterial Producer of Phosphorylated Nonpeptidic Antigens for Human $\gamma\delta$ T Cells. *Infect. Immun.* **1995**, *63*, 4628−4633.

(5) Dieli, F.; Troye-Blomberg, M.; Ivanyi, J.; Fournié, J. J.; Bonneville, M.; et al. Vγ9/Vδ2 T Lymphocytes Reduce the Viability of Intracellular *Mycobacterium tuberculosis*. *Eur. J. Immunol.* **2000**, *30*, 1512−1519.

(6) Dieli, F.; Troye-Blomberg, M.; Ivanyi, J.; Fournié, J. J.; Krensky, A. M.; et al. Granulysin-Dependent Killing of Intracellular and Extracellular *Mycobacterium tuberculosis* by Vγ9/Vδ2 T Lymphocytes. *J. Infect. Dis.* **2001**, *184*, 1082−1085.

(7) Shen, Y.; Zhou, D.; Qiu, L.; Lai, X.; Simon, M.; et al. Adaptive Immune Response of Vγ2/Vδ2$^+$ T Cells During Mycobacterial Infections. *Science* **2002**, *295*, 2255−2258.

(8) Elloso, M. M.; van der Heyde, H. C.; vande Waa, J. A.; Manning, D. D.; Weidanz, W. P. Inhibition of *Plasmodium falciparum* In Vitro by Human $\gamma\delta$ T Cells. *J. Immunol.* **1994**, *153*, 1187−1194.

(9) Poquet, Y.; Kroca, M.; Halary, F.; Stenmark, S.; Peyrat, M.-A.; et al. Expansion of Vγ9/Vδ2 T Cells Is Triggered by *Francisella tularensis*-Derived Phosphoantigens in Tularemia but Not after Tularemia Vaccination. *Infect. Immun.* **1998**, *66*, 2107−2114.

(10) Das, H.; Wang, L.; Kamath, A.; Bukowski, J. F. Vγ2/Vδ2 T-Cell Receptor-Mediated Recognition of Aminobisphosphonates. *Blood* **2001**, *98*, 1616−1618.

(11) Miyagawa, F.; Tanaka, Y.; Yamashita, S.; Minato, N. Essential Requirement of Antigen Presentation by Monocyte Lineage Cells for the Activation of Primary Human $\gamma\delta$ T Cells by Aminobisphosphonate Antigen. *J. Immunol.* **2001**, *166*, 5508−5514.

(12) Kato, Y.; Tanaka, Y.; Miyagawa, F.; Yamashita, S.; Minato, N. Targeting of Tumor Cells for Human $\gamma\delta$ T Cells by Nonpeptide Antigens. *J. Immunol.* **2001**, *167*, 5092−5098.

(13) Kunzmann, V.; Bauer, E.; Feurle, J.; Weiβinger, F.; Tony, H.-P.; et al. Stimulation of $\gamma\delta$ T Cells by Aminobisphosphonates and Induction of Antiplasma Cell Activity in Multiple Myeloma. *Blood* **2000**, *96*, 384−392.

(14) Sicard, H.; Al Saati, T.; Delsol, G.; Fournié, J. J. Synthetic Phosphoantigens Enhance Human Vγ9/Vδ2 T Lymphocytes Killing of Non-Hodgkin's B Lymphoma. *Mol. Med.* **2001**, *7*, 711−722.

(15) Wilson, I. A.; Stanfield, R. L. Unraveling the Mysteries of $\gamma\delta$ T Cell Recognition. *Nat. Immunol.* **2001**, *2*, 579−581.

(16) Belmant, C.; Espinosa, E.; Halary, F.; Tang, Y.; Peyrat, M.-A.; et al. A Chemical Basis for Recognition of Nonpeptide Antigens by Human $\gamma\delta$ T Cells. *FASEB J.* **2000**, *14*, 1669.

(17) Espinosa, E.; Belmant, C.; Sicard, H.; Poupot, R.; Bonneville, M.; et al. Y2K+1 State-of-the-Art on Non-Peptide Phosphoantigens, A Novel Category of Immunostimulatory Molecules. *Microbes Infect.* **2001**, *3*, 645−654.

(18) Morita, C. T.; Lee, H. K.; Wang, H.; Li, H.; Mariuzza, R. A.; et al. Structural Features of Nonpeptide Prenyl Pyrophosphates that Determine their Antigenicity for Human $\gamma\delta$ T Cells. *J. Immunol.* **2001**, *167*, 36−41.

(19) Bukowski, J. F.; Morita, C. T.; Brenner, M. B. Human $\gamma\delta$ T Cells Recognize Alkylamines Derived from Microbes, Edible Plants, and Tea: Implications for Innate Immunity. *Immunity* **1999**, *11*, 57−65.

(20) Tanaka, Y.; Sano, S.; Nieves, E.; De Libero, G.; Rosa, D.; et al. Nonpeptide Ligands for Human $\gamma\delta$ T Cells. *Proc. Natl. Acad. Sci. U.S.A.* **1994**, *91*, 8175−8179.

(21) Jomaa, H.; Feurle, J.; Lühs, K.; Kunzmann, V.; Tony, H.-P.; et al. Vγ9/Vδ2 T Cell Activation Induced by Bacterial Low Molecular Mass Compounds Depends on the 1-Deoxy-D-Xylulose 5-Phosphate Pathway of Isoprenoid Biosynthesis. *FEMS Immunol. Med. Microbiol.* **1999**, *25*, 371−378.

(22) Feurle, J.; Espinosa, E.; Eckstein, S.; Pont, F.; Kunzmann, V.; et al. *Escherichia coli* Produces Phosphoantigens Activating Human $\gamma\delta$ T Cells. *J. Biol. Chem.* **2002**, *277*, 148−154.

(23) Behr, C.; Poupot, R.; Peyrat, M.-A.; Poquet, Y.; Constant, P.; et al. *Plasmodium falciparum* Stimuli for Human $\gamma\delta$ T Cells are Related to Phosphorylated Antigens of Mycobacteria. *Infect. Immun.* **1996**, *64*, 2892−2896.

(24) Hintz, M.; Reichenberg, A.; Altincicek, B.; Bahr, U.; Gschwind, R. M.; et al. Indentification of (*E*)-4-hydroxy-3-methyl-but-2-enyl Pyrophosphate as a Major Activator for Human $\gamma\delta$ T Cells in *Escherichia coli*. *FEBS Lett.* **2001**, *509*, 317−322.

(25) Morita, C. T.; Lee, H. K.; Samuelson, M.; Märker-Hermann, E.; Pasa-Tolic, L.; et al. Human $\gamma\delta$ T Cells Recognize an Intermediate in Bacterial Isoprenoid Metabolism: Pattern Recognition by the Adaptive Immune System. *Department of Internal Medicine Research Day*; University of Iowa, 2002. http://www.int-med.uiowa.edu/research/ResearchDay/AbstractsC.html#C2.

(26) *Cerius² Modeling Environment*, Version 4.5; Accelrys Inc.: San Diego, CA.

(27) *Catalyst*, Version 4.6; Molecular Simulations Inc.: Burlington, MA.

(28) Szabo, C. M.; Oldfield, E. An Investigation of Bisphosphonate Inhibition of a Vacuolar Proton-Pumping Pyrophosphatase. *Biochem. Biophys. Res. Commun.* **2001**, *287*, 468−473.

(29) Szabo, C. M.; Matsumura, Y.; Fukura, S.; Martin, M. B.; Sanders, J. M.; et al. Inhibition of Geranylgeranyl Diphosphate Synthase by Bisphosphonates and Diphosphates: A Potential Route to New Bone Antiresorption and Antiparasitic Agents. *J. Med. Chem.* **2002**, *45*, 2185−2196.

(30) Tanaka, Y.; Morita, C. T.; Tanaka, Y.; Nieves, E.; Brenner, M. B.; et al. Natural and Synthetic Non-Peptide Antigens Recognized by Human $\gamma\delta$ T Cells. *Nature* **1995**, *375*, 155−158.

(31) Belmant, C.; Espinosa, E.; Poupot, R.; Peyrat, M.; Guiraud, M.; et al. 3-Formyl-butyl Pyrophosphate a Novel Mycobacterial Metabolite Activating Human $\gamma\delta$ T Cells. *J. Biol. Chem.* **1999**, *26*, 32079−32084.

(32) Belmant, C.; Fournié, J.-J.; Bonneville, M.; Peyrat, M. A. Nouveaux composés phosphohalohydrines, procède de fabrication et applications. Fr. Patent 2,782,721, 1998.

(33) Hasegawa, K.; Funatsu, K. Partial Least Squares Modeling and Genetic Algorithm Optimization in Quantitative Structure−Activity Relationships. *SAR QSAR Environ. Res.* **2000**, *11*, 189−209.

(34) Gasteiger, J.; Marsili, M. Iterative Partial Equalization of Orbital Electronegativity−A Rapid Access to Atomic Charges. *Tetrahedron* **1980**, *36*, 3219−3288.

(35) Cramer, R. D.; Bunce, J. D.; Patterson, D. E.; Frank, I. E. Crossvalidation, Bootstrapping, and Partial Least Squares Compared with Multiple Regression in Conventional QSAR Studies. *Quant. Struct.-Act. Relat.* **1988**, *7*, 18−25.

(36) Allison, T. J.; Winter, C. C.; Fournié, J. J.; Bonneville, M.; Garboczi, D. N. Structure of a Human T-cell Antigen Receptor. *Nature* **2001**, *411*, 820−824.

(37) Poccia, F.; Battistini, L.; Cipriani, B.; Mancino, G.; Martini, F.; et al. Phosphoantigen-Reactive Vγ9/Vδ2 T Lymphocytes Suppress In Vitro Human Immunodeficiency Virus Type 1 Replication by Cell-Released Antiviral Factors Including CC Chemokines. *J. Infect. Dis.* **1999**, *180*, 858−861.

(38) Gonzalez-Aseguinolaza, G.; Van Kaer, L.; Bergmann, C. C.; Wilson, J. M.; Schmieg, J.; et al. Natural Killer T Cell Ligand α-Galactosylceramide Enhances Protective Immunity Induced by Malaria Vaccines. *J. Exp. Med.* **2002**, *195*, 617−624.